Energy, Mines and Resources Canada
Énergie, Mines et Ressources Canada

CANMET
Canada Centre for Mineral and Energy Technology
Centre canadien de la technologie des minéraux et de l'énergie

MINERALOGICAL AND PETROLOGICAL CHARACTERIZATION OF HOST ROCKS AND TAILINGS SAMPLES FROM LES MINES SELBAIE, NORTHERN QUEBEC

J.L. Jambor
Environmental Laboratory

D.R. Owens and R. Lastra
Core Technologies and Services Laboratory

June 1992

Project: 30.14.99
Co-disposal of Tailings and Waste Rocks in Basins

This document is an unedited interim report prepared primarily for discussion and internal reporting purposes. It does not represent a final expression of the opinion of the Canada Centre for Mineral and Energy Technology (CANMET)

Ce document est un rapport provisoire non-révisé et rédigé principalement pour fin de discussion et de documentation interne. Il ne représente nullement l'expression définitive de l'opinion du Centre canadien de la technologie des minéraux et de l'énergie (CANMET)

32 pp

MINERAL SCIENCES LABORATORIES
DIVISION REPORT MSL 92-41 (IR)

Crown Copyrights Reserved

MICROMEDIA

92-06279/

MINERALOGICAL AND PETROLOGICAL CHARACTERIZATION OF HOST ROCKS AND TAILINGS SAMPLES FROM LES MINES SELBAIE, NORTHERN QUEBEC

by

J.L. Jambor*
Environmental Laboratory

D.R. Owens** and R. Lastra**
Core Technologies and Services Laboratory

ABSTRACT

Petrographic and mineralogical studies of waste rocks and tailings samples from the Selbaie mine, northern Quebec, indicate that pervasive silicification has occurred and that the non-sulphide assemblage consists almost wholly of quartz, chlorite, and muscovite ± carbonates. The principal sulphides in the samples are pyrite ± sphalerite ± chalcopyrite; pyrrhotite and potential sources of deleterious elements, such as arsenic-bearing minerals, are present but seem to be too sparse to be of significant environmental concern. Thus, within the four waste rock types and two tailings types examined in the study, pyrite alone would account for nearly all of the potential acid generation. Carbonate contents and compositions are highly variable in the rocks and tailings. Dolomite is the most abundant carbonate, followed by siderite, and quantitative electron microprobe analyses show that Fe-Mg-Mn solid solution is extensive in both. Rhyodacitic breccia contains > 10% dolomite,

Keywords: waste rocks, altered volcanics, mineralogy, pyrite, carbonates, acid mine drainage, tailings, Selbaie mine, Quebec.

---

* Environmental Labaoratory, ** Core Technologies and Services Laboratory, Mineral Sciences Laboratories, CANMET, Energy, Mines and Resources Canada, Ottawa, Ontario, K1A 0G1.

which is the highest abundance of carbonate minerals in the four rock types (welded andesite tuff, intermediate volcanics, rhyodacitic breccia, pyrite-rich waste rock). The distinction between the as-received iron-rich and iron-poor tailings seems to be related directly to pyrite content. The tailings contain dolomite, ankerite and siderite and in terms of the mitigation of acid mine drainage, the pyrite-poor tailings and the carbonate-rich waste rock are the best potential local sources of material to abate future acid generation and migration.

INTRODUCTION

The Selbaie mine (Les Mines Selbaie), which in its earlier years was known as the Detour deposit (Deptuck et al., 1982), is about 180 km north of Noranda and about 80 km northwest of Joutel in northern Quebec. The deposit was discovered in 1974 by ground follow-up of an anomaly detected a year or two earlier by an airborne electromagnetic survey. Drilling in 1974-1975 outlined 25-29 million tonnes of ore in three zones, of which the largest is the open-pit A-1 zone originally containing 20 million tonnes grading 0.8% Cu, 2.2% Zn, 31 g Ag/t, and 0.5 g Au/t (Bryce 1990). The mine came into production in 1981 using ore from the B zone, which contained 3.5 million tonnes grading 3.3% Cu, 30 g Ag/t, 1 g Au/t, and Zn as non-recoverable sphalerite coated with chalcocite (Bryce 1990). The mine currently operates at about 7200 tpd, with ore drawn from the A-1 open-pit zone, and from underground mines in the other two zones. Specific production figures and updated reserves for the zones are given by Wood and Duval (1990) and Bouillon (1990).

Purpose of Study

A mineralogical study of rocks and tailings from the Selbaie mine was undertaken as a component of a broader CANMET investigation to evaluate whether acid mine drainage from Selbaie waste rock can be neutralized or minimized by combining this rock with the available non-reactive sulphide tailings; different tailings - rock combinations are deposited into variously engineered storage basins, and these repositories are monitored to assess reactions and the quality and quantity of effluents. The project involving basinal co-deposition of waste rocks and tailings for the arrest or amelioration of AMD is identified within CANMET as the "co-disposal" of these wastes.

MATERIALS

The material provided by Selbaie via P. Friedrich of CANMET consisted of two plastic sample bags filled with tailings, and eight similar bags containing numerous hand specimens whose megascopic and microscopic features are described in Appendix A. The hand specimens were collected in October 1991, and the eight bags were assembled at the minesite to represent four major waste-rock types as follows:

co-disposal 1: welded andesitic tuff;
co-disposal 2: intermediate volcanics;
co-disposal 3: rhyodacitic breccia; and
co-disposal 5: pyrite-rich waste rock.

Weight of each of the above four sample types was >5 kg. The two tailings samples (co-disposal 6 and 7) represent tailings that were collected in batches weighing from 21 to 100 g, over the period September 11-22, 1991 to make up composites having low and high iron contents (5.81 and 9.51 wt% Fe, respectively). Each of these tailings composite samples weighed 1.5 kg. Descriptions of the hand specimens in Appendix A are in the past tense because, other than portions of specimens that were removed for thin and polished sections (and for megascopic reference), the hand specimens were ground to 100% minus 150 mesh (aperture size 106 micrometres); thus, after grinding, the two bags of original material representing each sample type were combined and blended into a single homogeneous product for use in X-ray diffractometry, image analysis, and other tests.

RESULTS

Optical Microscopy

The microscopy studies as outlined in Appendix A indicate that the rocks are silicified volcanics with a relatively simple mineralogy that is notable for its absence of feldspars.

Excluding the sulphide minerals, all of the rocks contain at least 50% quartz, and all contain several percent muscovite and chlorite; no other minerals occur persistently at these abundances. Thin-section studies indicate that carbonate minerals are locally a major constituent, but their occurrence in quantity is somewhat erratic.

The sulphides are mainly pyrite, with sphalerite next in abundance, and then chalcopyrite. A few blebs of pyrrhotite in pyrite were observed, but quantitatively the blebs are of no consequence. Some of the rocks contain goethite and narrow rims and thin veinlets of supergene chalcocite locally accompanied by covellite, digenite, and marcasite (Figs. 1, 2, 3). One section was found to contain native silver and a complex intergrowth of tetrahedrite and an Ag-Cu-Sb-S phase (Fig. 4); the unidentified phase may be polybasite, which was reported by Sinclair and Gasparrini (1980) to occur at Selbaie.

X-ray Diffractometry

After grinding and homogenization, each of the four rock samples (co-disposal 1, 2, 3 and 5) was examined using a Rigaku rotating anode X-ray powder diffractometer. The resultant diffractograms and identification of the peaks are shown in Figures 5 and 6, and the relative proportions of the minerals in the rocks and in the tailings samples are listed in Table 1. The results show that quartz, chlorite, and muscovite are abundant and pervasive in all rock types. Among the more prominent variations, pyrite is a major constituent of co-disposal 5, a minor constituent of 3, and is relatively low in 1 and 2. The main difference between the iron-poor and iron-rich tailings (co-disposal 6 and 7, respectively) is the higher pyrite content of the iron-rich sample. The as-received iron-rich sample was not completely homogeneous in that a small amount of lighter grey material was present; this material presumably reflects tailings variations during one or more of the nineteen individual sampling periods that were used to assemble the bulk sample. The diffractometer pattern of the lighter grey material (7W in Fig. 6) shows that this fraction contains less pyrite and more muscovite, chlorite, quartz and dolomite than does the bulk of the sample.

A significant variation among the samples is the presence of large amounts of dolomite in co-disposal 3, but not in the others (Fig. 5). To check for possible water-soluble minerals, and for the acid-soluble ones, diffractometer patterns were run for each of the samples after washing successively in water, dilute acetic acid, and hydrochloric acid. Treatment with acetic acid is a method of selective dissolution of calcite, whereas HCl removes all carbonates (Fig. 7). Comparison of the diffractogram in Figure 7 with those in Figures 5 and 6 leads to the following conclusions after observing the effects of the acid washes:

co-disposal 1:	no change; the X-ray peak at the dolomite position is an overlapping diffraction line from muscovite;
co-disposal 2:	no change, as above;
co-disposal 3:	presence of major amounts of dolomite confirmed by acid dissolution; and
co-disposal 5:	small amounts of dolomite present (no interference from overlapping X-ray line of mica).

Image-analysis Study

After grinding and homogenization of the four co-disposal rock types, a portion of each was mounted in a polished section to obtain mineral quantities by image analysis. Although the high-iron and low-iron tailings were ultimately combined, the two samples were kept separate for the image-analysis work.

The X-ray and optical microscopic observations were the basis for the mineral categories used in the image-analysis study (Table 2). Except for small amounts of a Fe-Al-Si phase detected in the image-analysis work, the image-analysis results were in accord with the predecessor mineralogy. The Fe-Al-Si phase was reported to range from 0.01 to 1.31 vol%, and to average 0.48% in the six samples. The highest value (1.31%) was obtained from co-disposal 7. Quantitative electron-microprobe analyses of the unidentified phase

(Table A-2) showed it to be a chlorite that is anomalously iron-rich relative to the main chlorite.

Difficulties were encountered in attempting to quantify the percentages of carbonate minerals in the assemblages. The grey level of dolomite overlaps with that of chlorite and muscovite, and both dolomite and siderite in the Selbaie samples are highly variable in cation composition. This variation in composition from grain to grain means that each grain has a different average atomic number, which in turn translates to a corresponding variation in the "grey" level of intensity recorded by the imaging system. Consequently, the images containing the dolomite, muscovite, siderite, and chlorite were distinguished by energy-dispersion analyses (EDX), whereby each particle larger than 7 μm in diameter was individually scanned and identified as dolomite, siderite, muscovite, or chlorite; the remainder of the grains was allocated to the more general groupings chlorite-muscovite-dolomite.

The percentages of dolomite per se (confirmed by EDX) in Table 2 indicate that only co-disposal 3 is rich in dolomite, and the only other samples containing $>1\%$ dolomite are co-disposal 6 (1.8%) and 7 (also 1.8%). These results differ somewhat from those of X-ray diffractometry (Table 1), but are in complete accord with the degree of effervescence observed during the attack by HCl. As for siderite per se (confirmed by EDX), its quantities are too low to be unequivocally observed on the diffractograms; the addition of the possible amounts of siderite in the less specific "siderite-chlorite" category (Table 2) does not alter this relationship.

The "chlorite-muscovite-dolomite" category is significant in that percentages for the individual samples range from 2.7 to 11.5 vol%. The latter value is for co-disposal 1, but the X-ray diffractogram (Fig. 1) indicates that dolomite itself is not a significant component in this category for this sample. It seems likely that the percentages for dolomite and other minerals within the chlorite-muscovite-dolomite fines would roughly parallel the amounts present in the coarser fraction.

Electron-microprobe Analyses

Microprobe compositions were determined for the carbonates in polished thin sections of specimens from co-disposal 1, 2, and 3, and in polished sections of co-disposal 5 (crushed and homogenized final sample) and co-disposal 7 (tailings). The analytical results and cation formula percentages for the analyzed carbonates are given in Table 3.

The petrographic studies (Appendix A) and X-ray diffractograms (Figs. 5, 7) indicate that little carbonate is present in co-disposal 1. Most of the carbonate observed is in association with quartz and sphalerite in veinlets about 1 mm wide. The carbonate grains are zoned and vary in composition from smithsonite (i.e., Zn-dominant) to siderite (Fe-dominant), both of which are extremely manganese-rich (up to 11.7 wt% MnO).

In co-disposal 2 the carbonates occur both in quartz veinlets and as disseminations throughout the rock matrix. The carbonate in individual rock specimens was estimated to be as high as 5-6%. All of the "major" grains analyzed by microprobe are rich in magnesium and manganese (Table 3, where 2A and 2B are polished thin sections from separate hand specimens). These large, relatively abundant carbonate grains account for more than 90% of the total carbonate, and most of the remainder is present as small inclusions within the larger grains. The compositions of the inclusions are conspicuously lower in magnesium and higher in manganese and iron relative to compositions of the host grains; nevertheless, that the inclusions and host both have the formula of siderite is surprising in light of the unlimited Fe-Mg-Mn solid solution. Phenomena such as incomplete replacement and recrystallization could be invoked to account for the bimodal siderite compositions, but this aspect and other possible explanations were not pursued as they are not particularly relevant to the present study.

Co-disposal 3 differs from the other rocks in that the carbonate content is high, and the abundance is confirmed by all determinative methods: optical microscopy, X-ray diffraction, acid-dissolution tests, and image analyses. The image-analysis results indicate

that the siderite content is negligible, and dolomite amounts to at least 12.4 vol% (Table 2). Microprobe analyses of the dolomite show that iron and manganese substitution is relatively low, totalling less than 20% of the magnesium position (Table 3).

The carbonate content of co-disposal 5 is low, and this sample is highly enriched in sulphides (Table 2). Dolomite is the principal carbonate, but siderite and magnesite are also present (Table 3). Microprobe analyses indicate that the siderite-magnesite ($FeCO_3$-$MgCO_3$) compositions are extremely varied in cation substitutions; dolomite also shows a fair range of Fe-Mg solid solution, but all compositions are well within the field of dolomite proper, i.e., formula Mg > Fe (Table 3).

Tailings sample co-disposal 7 contains a moderate amount of carbonate (Tables 1 and 2). Microprobe analyses indicate that the main phase is of the dolomite type, but compositions extend from dolomite to well into the field of ankerite. The two analyses of siderite (Table 3) show substantial differences in manganese content and Fe-Mg substitution. Siderite compositions of grains separated into a heavy-liquid sink fraction show an even greater variation: individual grains have been found in which manganese is present and magnesium negligible; also noted was a grain having similar amounts of manganese and zinc, and negligible magnesium.

CONCLUSIONS

Mineralogical and petrographic studies of the co-disposal rocks indicate that they are predominantly tuffs that have been extensively silicified and metamorphosed to a simple assemblage consisting overwhelmingly of quartz, chlorite, and muscovite. Both within the waste rock and the tailings, pyrite is the principal sulphide mineral; pyrrhotite occurs only in trace amounts, always as bleb inclusions in pyrite, and thus is not a factor in acid generation at Selbaie mines. The principal variables in terms of acid generation and acid neutralization at Selbaie mine therefore can be simplified by considering pyrite to be the acid generator, and carbonates to be the acid neutralizers.

Quantification of the mineral contents of the co-disposal samples can in large part be determined by chemical partitioning as follows:

1. Pb as galena, Zn as sphalerite (microprobe analyses indicate an iron content of < 1 wt%), and Cu as chalcopyrite; the remainder of sulphide sulphur can be allocated to pyrite.
2. Total carbonate as dolomite or dolomite plus siderite, depending on the rock type. For tailings, the dolomite:siderite ratio could be taken as 5:1. The CO_2 contents for $FeCO_3$ and $MnCO_3$ are similar (38.0 and 38.3 wt%), whereas that of $MgCO_3$ is 52.2 wt%. Partitioning of (Fe + Mn):Mg is necessary, and is probably best done using the rock types as a crude guideline. Pure dolomite contains 47.7 wt% CO_2, whereas ankerite with Fe $\geq$ Mg (i.e., $\sim$1:1) contains 44.0%; mid-point compositions therefore would have about 45.8% CO_2.

In terms of rock types, the pyrite-rich waste (co-disposal 5) obviously would be the most significant acid generator, and the so-called rhyodacitic breccia (co-disposal 5) has the best capacity to neutralize acidity and precipitate iron oxyhydroxides. For the tailings samples, the one lower in iron is primarily a manifestation of a lower pyrite content, with obvious implications as to acid-generating consequences. For the co-disposal of waste rocks and/or tailings, various scenarios of layering of materials can be envisaged. It would seem, however, that a simple sandwich-type arrangement, in which carbonate-rich material underlies and overlies pyrite-rich waste, should be effective.

ACKNOWLEDGEMENTS

The authors are grateful to P. Carrière, J.M. Beaulne, and J.M. Greer for technical assistance, and to P. Friedrich for providing the samples.

REFERENCES

1. Bouillon, J.J. (1990). Les Mines Selbaie story: geology. Bull. Can. Inst. Mining Metall. Petrol. **83**, No. 936, 79-82.

2. Bryce, R.C. (1990). Les Mines Selbaie story: introduction. Bull. Can. Inst. Mining Metall. Petrol. **83**, No. 936, 73-76.

3. Deptuck, R., Squair, H. and Wierzbicki, V. (1982). Geology of the Detour zinc-copper deposits, Brouillan Township, Quebec. In Precambrian Sulphide Deposits, H.S. Robinson Memorial Volume (R.W. Hutchinson, C.D. Spence, J.M. Franklin, eds.), Geol. Assoc. Can. Special Paper 25, 319-342.

4. Wood, K. and Duval, L. (1990). Les Mines Selbaie story: concentrator development and operation. Bull. Can. Inst. Mining Metall. Petrol. 83, No. 936, 94-100.

Table 1. Relative proportions of minerals as indicated by X-ray diffractometry

Sample	ch	mu	tc	q	py	DOL	effervescence in acid
Co-disp. 1	M	M	-	M	w	w	extremely weak
Co-disp. 2	M	M	-	M	-	w	slight but clearly positive
Co-disp. 3	M	m	w	M	m	M	strong
Co-disp. 5	M	w	-	M	M	w	extremely weak
Co-disp. 6	M	m	-	M	w	w	slight, but stronger than #2
Co-disp. 7W	M	m	-	M	w	w	----
Co-disp. 6 & 7	M	m	-	M	w	w	moderate, still active after 1 hour
Co-disp. 7	M	m	-	M	w	M	strong, second only to co-disp. 3

ch chlorite, mu muscovite, tc talc, q quartz, py pyrite, DOL dolomite

M major, m minor (5-10%), w (0.5-5%); percentages indicate relative magnitudes and are not intended to denote quantitative values.

Co-disposal 1, 2, 3, 5:	major waste-rock types
Co-disposal 6:	tailings sample, low-iron type (5.81 wt% Fe)
Co-disposal 7W:	lighter grey component in as-received tailings sample co-disposal 7
Co-disposal 6 + 7:	final product after blending of co-disposal 6 and co-disposal 7
Co-disposal 7:	representative of bulk of co-disposal 7 (high-iron tailings, in this case containing 9.51 wt% Fe).

Table 2. Image-analysis results for co-disposal samples

Co-disposal	1		2		3		5		6		7	
	wt%	vol%	wt%	vol%	wt%	vol%	wt%	vol%	wt%	vol%	wt%	vol%
quartz	57.2	62.6	74.8	78.3	47.7	55.9	15.9	25.1	79.5	83.4	74.8	81.6
chlorite	12.4	12.0	10.2	9.4	8.8	9.1	4.0	5.6	6.1	5.7	2.5	2.4
Fe-rich chl.	0.3	0.2	1.3	0.9	0.1	0.1	--	-0.6	0.4	2.0	1.3	
muscovite	5.3	5.3	4.2	4.0	0.6	0.7	0.6	0.9	0.6	0.4	1.2	1.2
pyrite	8.0	4.6	2.3	1.3	24.0	14.8	75.7	63.3	6.2	3.4	13.2	7.6
chalcopyrite	1.8	1.2	0.6	0.4	1.6	1.2	<0.1	<0.1	<0.1	<0.1	<0.1	<0.1
sphalerite	2.4	1.7	0.3	0.2	0.6	0.4	1.2	1.3	0.2	0.1	0.6	0.4
galena	0.06	0.02	0.08	0.03	0.12	0.05	0.00	0.00	0.01	0.00	0.02	0.01
ch-mu-dol*	11.6	11.6	4.7	4.5	5.0	5.4	2.4	3.5	3.8	3.7	2.7	2.7
dolomite	0.4	0.4	0.1	0.1	11.4	12.4	0.2	0.3	1.5	1.5	1.8	1.8
siderite	0.3	0.2	1.3	0.9	<0.1	<0.1	<0.1	<0.1	0.3	0.2	0.3	0.2
siderite Fe-rich chl.**	0.3	0.2	0.1	<0.1	0.1	0.1	<0.1	<0.1	0.2	0.2	1.0	0.7

*remainder of particles from chlorite-muscovite-dolomite image; all are smaller than 7 μm
**remainder of particles from siderite - Fe-rich chlorite image; all are smaller than 7 μm.

Table 3. Electron-microprobe analyses of Selbaie carbonates

Co-disposal 1

		zoned				zoned		
		(a)	(b)	(c)	(d)	(a)	(b)	(c)
wt%	Fe	17.5	19.3	22.9	26.8	20.6	35.5	40.7
	Zn	25.7	23.7	20.5	11.7	24.6	0.6	0.6
	Mn	4.4	5.5	4.5	8.5	3.8	9.1	4.9
	Ca	0.2	0.3	0.2	0.5	0.2	1.7	1.1
	Mg	0.1	0.1	0.1	0.2	0.0	0.7	0.7
mol	Fe	36.3	40.0	47.5	55.6	42.7	73.7	84.4
	Zn	49.3	45.5	39.3	22.4	47.2	1.2	1.2
	Mn	9.2	11.5	9.4	17.8	7.9	19.0	10.3
	Ca	0.5	0.7	0.5	1.2	0.5	4.2	2.7
	Mg	0.3	0.3	0.3	0.7	0.0	2.4	2.4
ident.		smith	smith	sid	sid	smith	sid	sid

Co-disposal 2A

		major phase 6 grains		major phase 5 grains		inclusions 4 grains		inclusions 5 grains	
		range	av.	range	av.	range	av.	range	av.
wt%	Fe	31.0-31.5	31.3	32.1-33.0	32.5	34.8-36.3	35.6	32.9-40.2	36.7
	Mn	2.6-3.9	3.6	2.6-4.3	3.3	7.1-8.2	7.6	4.0-9.1	7.2
	Ca	0.3-0.5	0.4	0.3-0.4	0.3	1.7-2.5	2.0	0.8-3.5	2.4
	Mg	7.2-7.7	7.4	7.2-7.9	7.6	0.7-0.9	0.8	0.7-1.5	1.2
mol	Fe		64.9		67.4		73.9		76.1
	Mn		7.5		6.9		15.9		15.1
	Ca		1.0		0.7		5.0		6.0
	Mg		25.7		26.4		2.8		4.2
ident.			sid		sid		sid		sid

Co-disposal 2B

		major phase 8 grains		major phase 4 grains		inclusions 4 grains		inclusions 3 grains	
		range	av.	range	av.	range	av.	range	av.
wt%	Fe	28.6-31.0	30.2	30.9-32.4	31.6	36.0-40.0	38.3	38.5-39.4	38.8
	Mn	3.3-4.3	3.8	2.5-4.2	3.6	5.5-7.8	6.5	6.1-6.3	6.2
	Ca	0.2-0.3	0.2	0.1-0.5	0.3	0.7-1.7	1.2	1.0-1.3	1.1
	Mg	7.2-8.6	7.8	7.4-8.1	7.7	0.4-0.9	0.6	0.5-0.9	0.7
mol	Fe		62.7		65.6		79.5		80.5
	Mn		7.9		7.5		13.6		13.0
	Ca		0.5		0.7		3.0		2.7
	Mg		27.1		26.7		2.1		2.4
ident.			sid		sid		sid		sid

Co-disposal 3

		major phase 5 grains		major phase 3 grains	
		range	av.	range	av.
wt%	Fe	2.6-3.1	2.8	3.0-3.4	3.2
	Mn	0.6-0.8	0.7	0.8-2.0	1.3
	Ca	19.8-20.6	20.2	21.1-21.8	21.3
	Mg	11.5-11.7	11.6	11.4-12.4	11.9
mol	Fe		5.8		6.6
	Mn		1.5		2.7
	Ca		50.5		53.2
	Mg		40.2		41.3
ident			dol		dol

Co-disposal 5

		grain 1	grain 2	grain 3	grain 4	grain 5	grain 6	grain 7	grain 8	grain 9
wt%	Fe	32.6	6.2	38.3	6.4	11.4	8.3	8.7	21.7	11.5
	Zn	0.0	0.0	0.0	0.0	0.0	0.0	0.0	0.0	0.0
	Mn	0.8	2.0	2.1	3.6	2.1	2.0	1.4	0.3	1.8
	Ca	0.2	20.5	3.0	21.1	20.8	20.8	19.7	0.4	20.5
	Mg	9.1	10.3	0.8	9.5	7.1	8.6	8.5	15.8	7.5
mol	Fe	67.6	12.9	79.5	13.3	23.7	17.2	18.0	45.0	23.9
	Zn	0.0	0.0	0.0	0.0	0.0	0.0	0.0	0.0	0.0
	Mn	1.7	4.1	4.4	7.5	4.4	4.2	2.9	0.6	3.8
	Ca	0.5	51.2	7.5	52.7	51.9	51.9	49.2	1.0	51.2
	Mg	31.6	35.7	2.8	33.0	24.6	29.8	29.5	54.8	26.0
ident.		sid	dol	sid	dol	dol	dol	dol	magn	dol

Co-disposal 7

		grain 1	grain 2	grain 3	grain 4	grain 5	grain 6	grain 7	grain 8
wt%	Fe	11.7	5.9	12.3	32.4	7.6	14.9	11.1	35.5
	Zn	0.0	0.0	0.0	0.0	0.0	0.0	0.0	0.0
	Mn	1.8	2.6	1.2	0.7	1.3	0.6	1.8	5.9
	Ca	19.4	20.6	19.8	0.3	20.1	19.3	20.5	0.0
	Mg	6.4	9.8	6.6	8.5	9.9	5.5	8.2	4.3
mol	Fe	24.3	12.2	25.5	67.2	15.8	30.9	23.0	73.7
	Zn	0.0	0.0	0.0	0.0	0.0	0.0	0.0	0.0
	Mn	3.8	5.4	2.5	1.5	2.7	1.3	3.8	12.3
	Ca	48.5	51.4	49.5	0.7	50.2	48.2	51.2	0.0
	Mg	22.2	34.0	22.9	29.5	34.3	19.1	23.6	14.9
ident.		ank	dol	ank	sid	dol	ank	dol	sid

smith smithsonite; sid siderite; dol dolomite; magn magnesite; ank ankerite

Figure 1. Matched pair of backscattered-electron images (left and right) with the right image showing pyrite (py) and sphalerite (sp), the latter with a rim of goethite (g, medium grey), in turn partly rimmed by secondary marcasite (m). Left image shows blebs of chalcopyrite (darker spots) in sphalerite, and thin veinlets of secondary chalcocite. Bar scale represents 100 μm.

Figure 2. Matched pair of backscatttered-electron (BSE) images showing pyrite (py), and sphalerite (sp) with "chalcopyrite disease". Left photo shows goethite (g, medium grey) coating on pyrite, and right photo shows chalcocite rim (white) on sphalerite. Bar scale represents 40 μm.

Figure 3. BSE image showing two large grains of delafossite (medium grey) containing irregular patches of chalcocite (white) and rims and veinlets of chalcocite that have extensively replaced pyrite (py). Bar scale represents 25 μm.

Figure 4. BSE image showing native silver (Ag) surrounded by quartz (black), sphalerite (sp), and chalcopyrite (cp). The grey phase intergrown with the silver is a heterogeneous mixture consisting of at least three minerals, one of which is probably argentian tetrahedrite (tt), and another is possibly polybasite. None of the minerals contains arsenic. Bar scale represents 25 μm.

Figure 5. X-ray diffractograms of co-disposal rock samples. Diffraction peaks correspond to the following: ch chlorite, mu muscovite, tc talc, q quartz, py pyrite, DOL dolomite, sid siderite. Dashed lines indicate positions of dolomite peaks.

Figure 6. X-ray diffractograms of co-disposal tailings samples: 6 is "low-iron" and 7 is "iron-rich" tailings as received; 7w is a light-coloured minor fraction from as-received 7; 6 + 7 is the final single sample after combining 6 and 7. Identification of peaks is as in Figure 5.

Figure 7. Diffractograms of co-disposal samples as in Figure 5, but after acid treatment. Residual peaks at the first DOL position are those of muscovite.

Figure 8. Diffractograms of acid-treated co-disposal samples; identifications as in Figures 5 and 6.

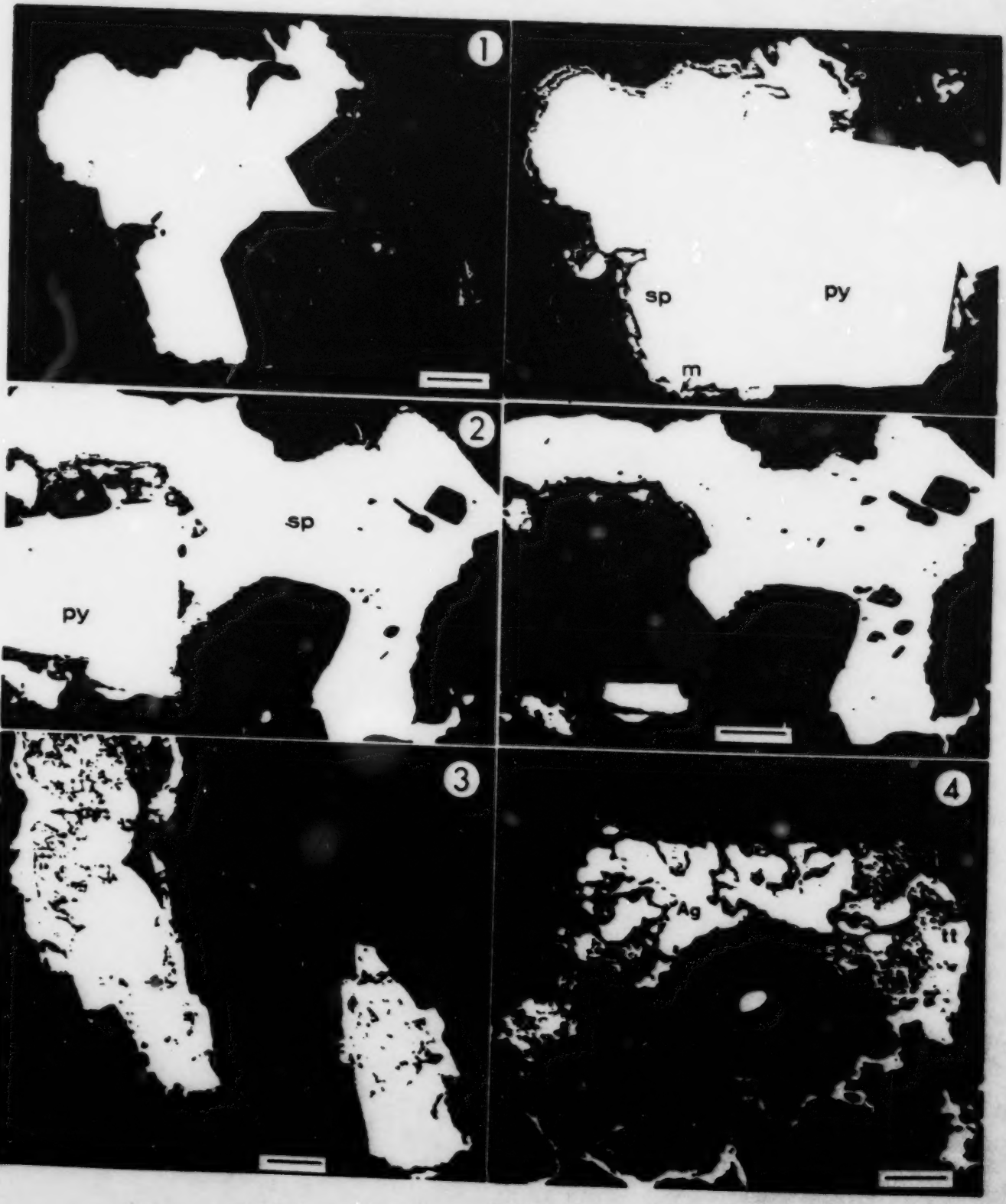
1
sp
py
m
2
sp
py
3
4
Ag
m

FIGURE 5

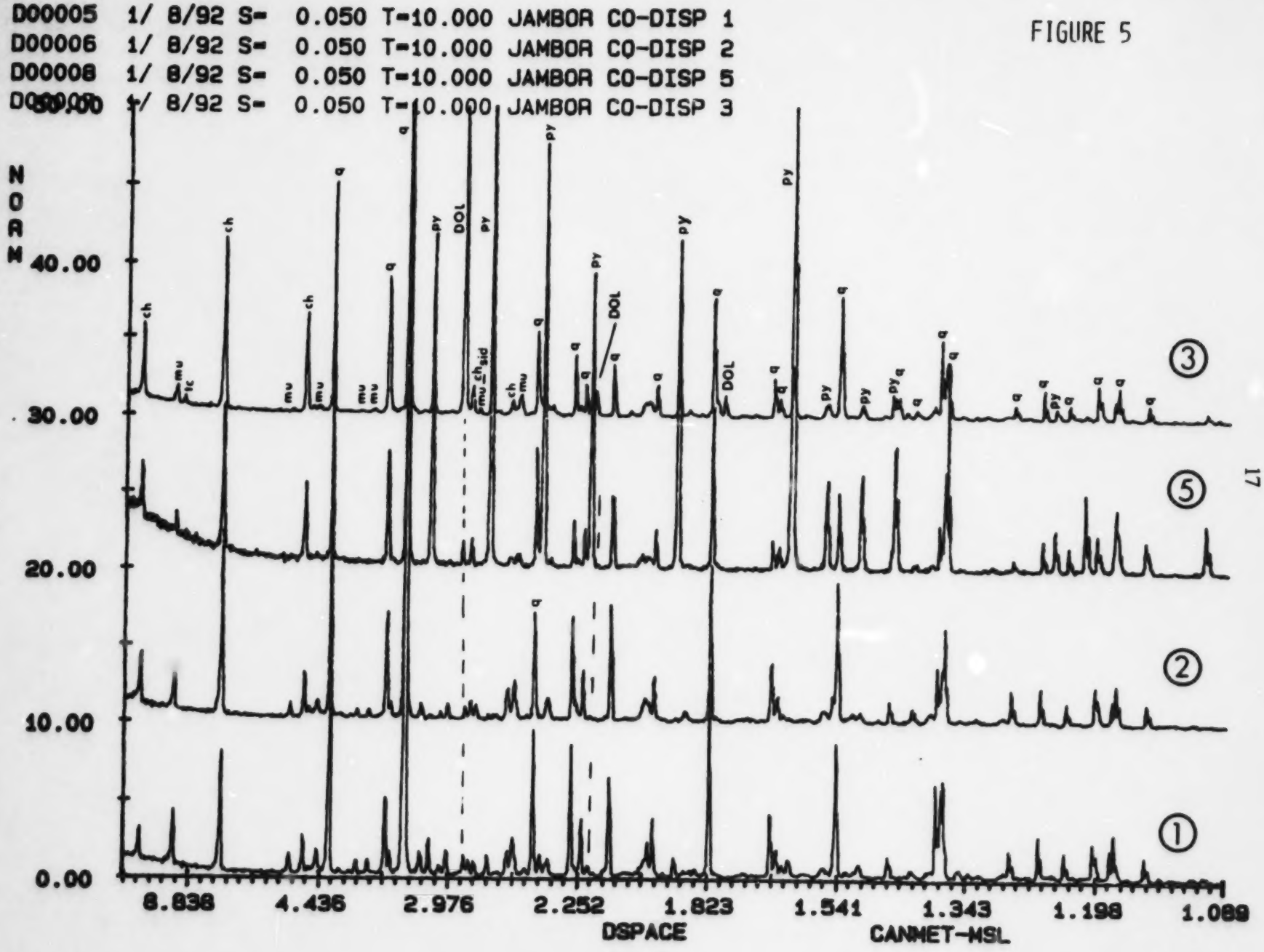
D00005 1/ 8/92 S= 0.050 T=10.000 JAMBOR CO-DISP 1
D00006 1/ 8/92 S= 0.050 T=10.000 JAMBOR CO-DISP 2
D00008 1/ 8/92 S= 0.050 T=10.000 JAMBOR CO-DISP 5
D00007 1/ 8/92 S= 0.050 T=10.000 JAMBOR CO-DISP 3
NORM
50.00
40.00
30.00
20.00
10.00
0.00
③
⑤
②
①
8.838
4.436
2.976
2.252
1.823
1.541
1.343
1.198
1.089
DSPACE
CANMET-MSL

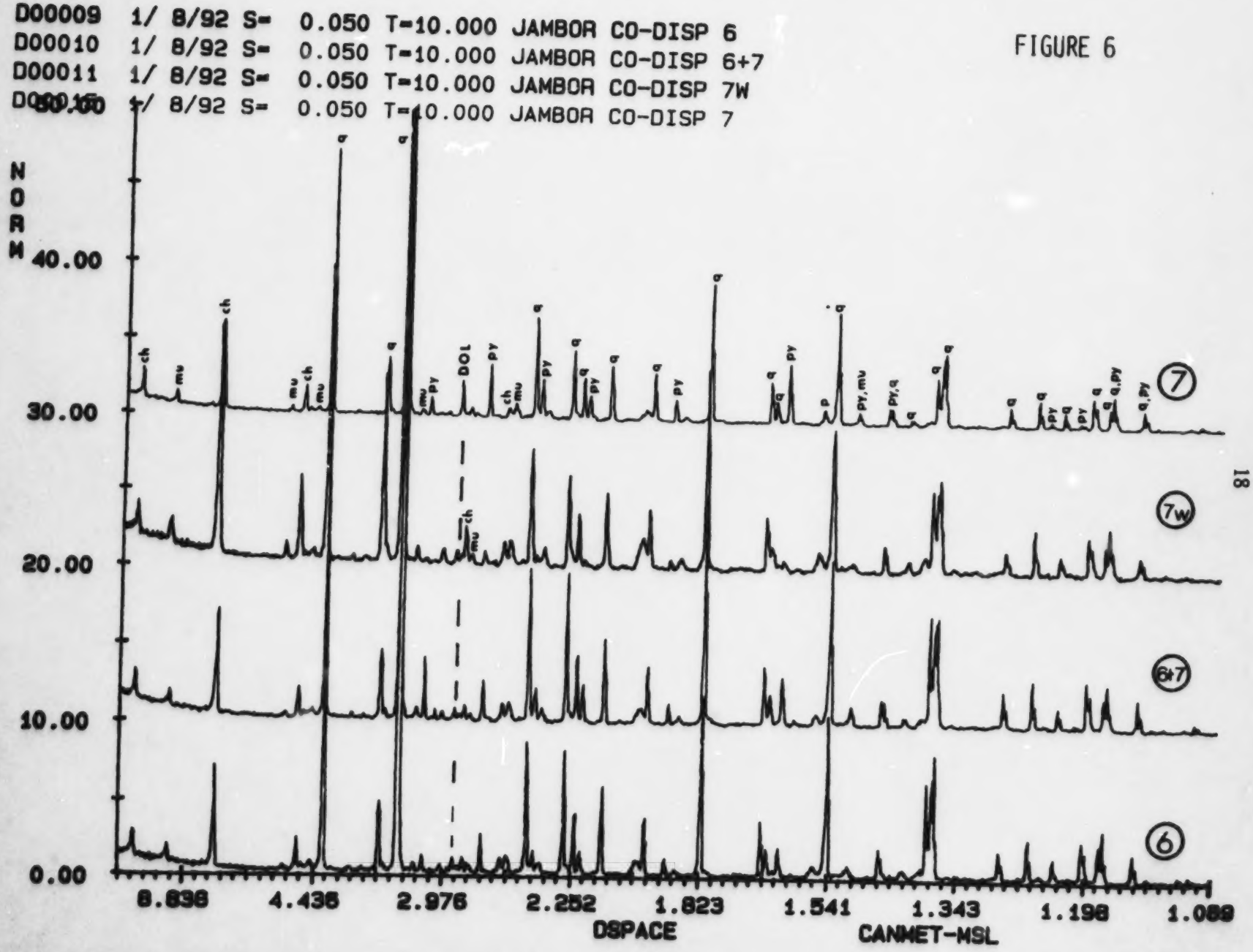
D00009 1/ 8/92 S= 0.050 T=10.000 JAMBOR CO-DISP 6
D00010 1/ 8/92 S= 0.050 T=10.000 JAMBOR CO-DISP 6+7
D00011 1/ 8/92 S= 0.050 T=10.000 JAMBOR CO-DISP 7W
D00012 1/ 8/92 S= 0.050 T=10.000 JAMBOR CO-DISP 7
NORM
40.00
30.00
20.00
10.00
0.00
7
7w
6+7
6
8.898
4.436
2.976
2.252
1.823
1.541
1.343
1.198
1.088
DSPACE
CANMET-MSL

FIGURE 6

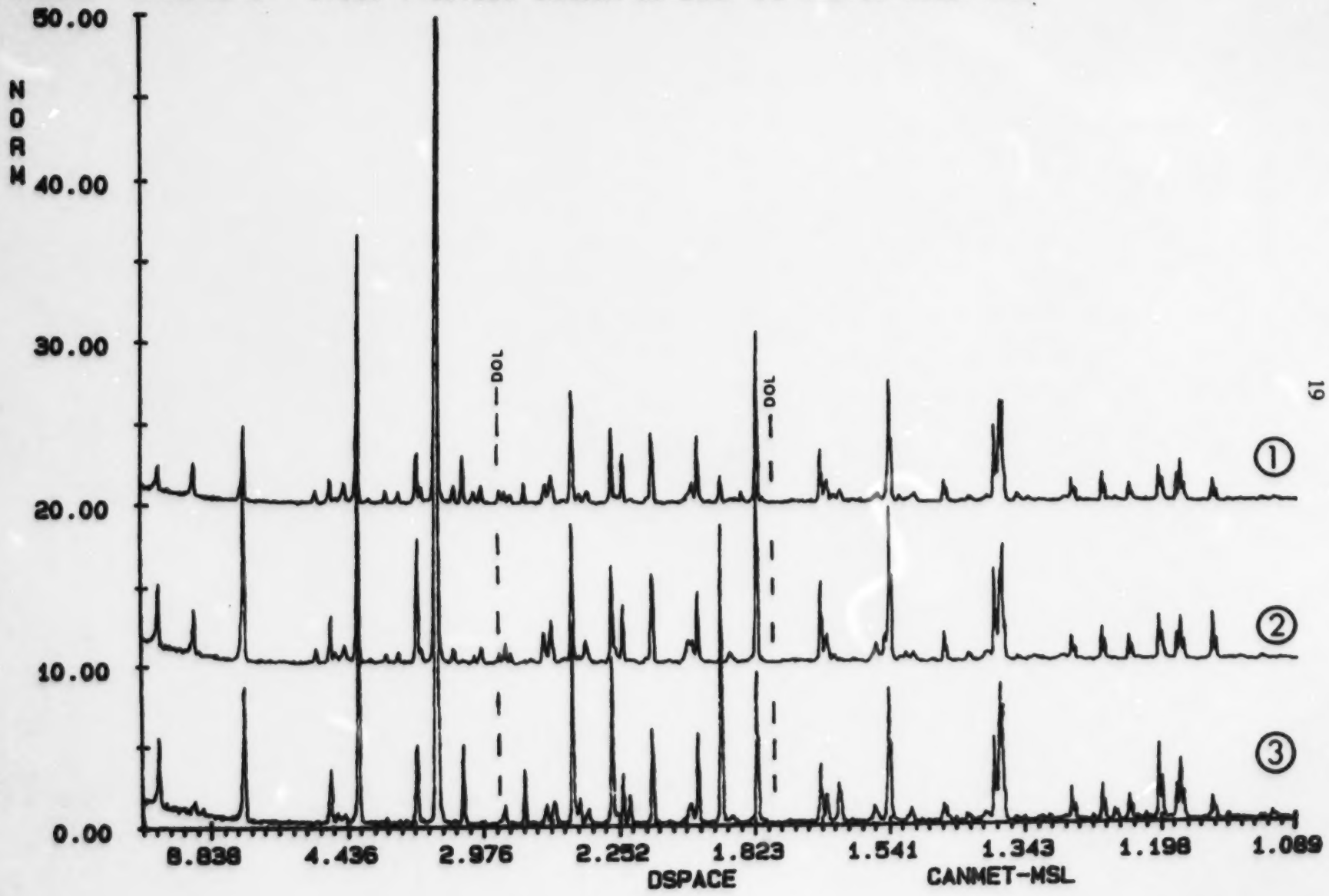
D00218 2/13/92 S= 0.050 T=10.000 JAMBOR CO-DISP #3 ACETIC ACID +HCL
D00217 2/13/92 S= 0.050 T=10.000 JAMBOR CO-DISP #2 ACETIC ACID +HCL
D00216 2/13/92 S= 0.050 T=10.000 JAMBOR CO-DISP #1 ACETIC ACID +HCL
50.00
NORM
40.00
30.00
20.00
10.00
0.00
DOL
DOL
①
②
③
8.838
4.436
2.976
2.252
1.823
1.541
1.343
1.198
1.089
DSPACE
CANMET-MSL
19
61

FIGURE 7

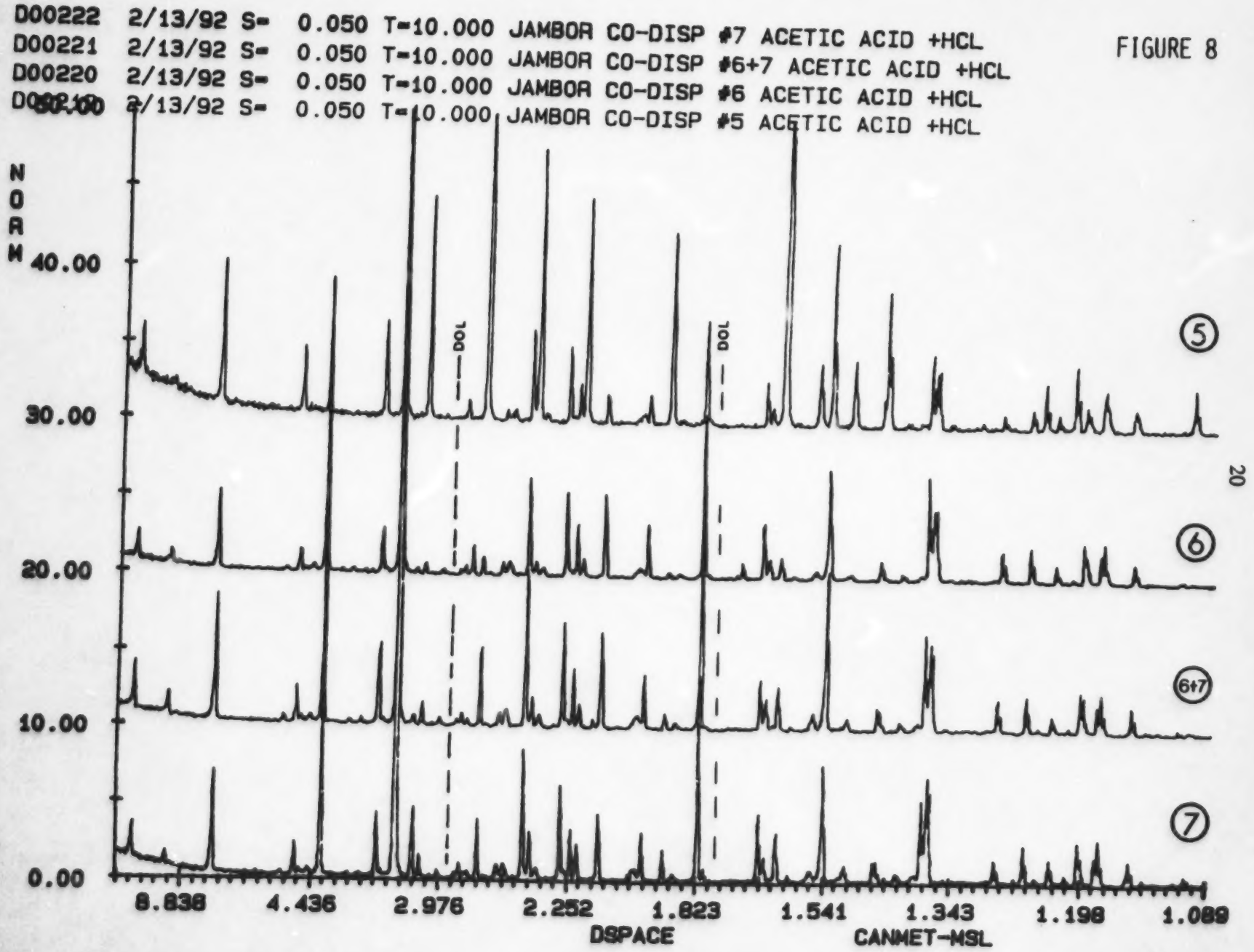
D00222 2/13/92 S= 0.050 T=10.000 JAMBOR CO-DISP #7 ACETIC ACID +HCL
D00221 2/13/92 S= 0.050 T=10.000 JAMBOR CO-DISP #6+7 ACETIC ACID +HCL
D00220 2/13/92 S= 0.050 T=10.000 JAMBOR CO-DISP #6 ACETIC ACID +HCL
D00219 2/13/92 S= 0.050 T=10.000 JAMBOR CO-DISP #5 ACETIC ACID +HCL
NORM
40.00
30.00
20.00
10.00
0.00
DOL
DOL
⑤
⑥
6+7
⑦
8.838
4.436
2.976
2.252
1.823
1.541
1.343
1.198
1.089
DSPACE
CANMET-MSL

FIGURE 8

Appendix A

Megascopic and Microscopic Descriptions of Samples

CO-DISPOSAL 1

(a) WAT 0-14

This bag of rocks and the succeeding one were provided as representing "welded andesitic tuff", which is presumably indicated by the labelling WAT; the numerical accompaniments (e.g., 0-14) for this and other samples apparently indicate a blast site in a trench.

The bag of specimens consisted of six pieces averaging about 12 x 6 x 4 cm, and several smaller pieces whose total volume was about two-thirds that of the larger pieces. The bulk of the material consisted of a greenish grey, very fine-grained volcanic rock containing irregular, black, chlorite-rich patches a few millimetres across, scattered throughout the rock and making up about 5% of it. Other pieces were similarly dark greenish grey and slightly foliated; although not chlorite-patched, the softness was assumed to indicate a substantial chlorite content. Fine-grained pyrite, some in euhedral cubes averaging 1 mm along an edge, was disseminated throughout the rocks; pyrite content averaged about 0.5%. Several fracture surfaces had yellowish brown to dark brown ochrous coatings, and these were identified as goethite by X-ray powder diffraction patterns.

(b) WAT 10-46

The bag contained 10 pieces of rock, each averaging about 4 x 6 x 9 cm, which were less foliated and more siliceous and sulphide-rich than WAT 0-14. In most of the specimens the sulphides were of the fine-grained disseminated type, and contents averaged $<1\%$; individual specimens, however, had up to 25% sulphides. Pyrite, chalcopyrite, and abundant sphalerite with small amounts of galena were identified; in the sulphide-rich specimens these minerals seemed to be present as highly irregular "veinlets" without sharp boundaries, presumably indicating a matrix-type occurrence rather than fracture control. A few irregular veinlets of mainly barren white quartz occurred in widths up to 1 cm.

Microscopy

Three polished thin sections and three polished sections were cut from the rocks making up co-disposal 1. One polished section shows about 0.8% fine-grained sulphides. Except for a large grain of sphalerite containing chalcopyrite blebs, and traces of chalcopyrite in a carbonate- and goethite-bearing quartz veinlet, the sulphides consist of pyrite averaging about 25 μm across. The sulphide content in the second polished section is about 5%, with more sphalerite than chalcopyrite or pyrite. Concentration of the sulphides, especially sphalerite, along fractures is pronounced. Rutile is common (but only ~1%), typically as clusters of anhedral grains associated with pyrite. The last of the three polished sections contains about 50% sulphides, nearly all of which are relatively coarse-grained sphalerite, chalcopyrite, and pyrite. Much of the sphalerite has "chalcopyrite disease", but the chalcopyrite blebs are relatively coarse (generally 1-3 μm). Galena is present in small amounts as scattered, angular, anhedral grains mainly in sphalerite.

One of the polished thin sections shows scattered subhedral to anhedral grains of pyrite to a maximum size of about 40 μm, and averaging about 25 μm; total volume of the pyrite is about 1%. The sawn face of the hand specimen shows two adjoining pyrite clusters, each about 0.5 x 1 cm and averaging about 50% pyrite in gangue. In the section for microscopy, individual crystals in these clusters are up to 1 mm across and appear to be prophyroblastic as evident from poikiloblastic inclusion arrays and triple-junction grain boundaries. Sulphide inclusions in the pyrite are mainly sphalerite, nearly all grains of which are more than 10 μm across, and most are much coarser. A few grains of chalcopyrite are present, and all are <900 μm^2. Pyrrhotite is relatively rare, occurring only as inclusions, typically <50 μm^2 and to a maximum of 1000 μm^2, in pyrite. Most of the sphalerite occupies interstices among pyrite grains, or adjoins pyrite grain boundaries. Several of the sphalerite grains are rimmed by chalcocite, some of which is accompanied by covellite and digenite that are in turn locally rimmed by goethite and marcasite (Fig. 1).

In transmitted light the rock is seen to consist mainly of a mosaic of fine-grained, equigranular, anhedral quartz containing abundant shreds of fine-grained muscovite and

chlorite. The matrix quartz averages < 10 μm in diameter, and is accompanied by sparse scattered phenocrysts of homogeneous quartz up to 1 mm across. The mica and chlorite show good alignment, and penetrative deformation is indicated by a conspicuous second alignment at an angle steeply obtuse to the main foliation. Grains of rutile and carbonate are locally present, as are quartz-chlorite-carbonate-sulphide veinlets up to 1 mm wide.

The apparent absence of feldspars is notable, and neither plagioclase nor K-feldspar is evident in the X-ray diffractogram (Fig. 5). The general features correspond fairly well with the "welded acid tuff" host rocks as described by Deptuck et al. (1982). Possibly the WAT designation on the sample labels signifies welded acid tuff rather than welded andesitic tuff.

CO-DISPOSAL 2

(a) INT 10-49

This bag and the next one were provided as representative of "intermediate" waste rock. Bag (a) contained ten pieces of rock, similar in size to those of co-disposal 1. The specimens were greenish black, darker than the WAT rocks and also more massive, lacking foliation. Numerous millimetre-wide quartz veinlets occurred, but the siliceous character of some of the rocks was evident mainly from the presence of several percent zoned, quartzose ovoids and patches, to 5 mm across, which typically have slightly to conspicuously diffuse margins. Several of the rock surfaces were iron-stained fracture faces. The sulphide minerals were disseminated and sparse ($< 1\%$) in all but the smallest specimen, which was 8 x 9 x 1.5 cm and contained an estimated 7% pyrite and chalcopyrite.

Three of the rock pieces were examined microscopically in three thin sections and in three polished sections. Two of the sections examined in reflected light are relatively sulphide-poor (3% and $< 1\%$ sulphides) and the other is sulphide rich (about 30%). Most of the sulphide grains are < 75 μm across and consist of chalcopyrite and subhedral to anhedral pyrite. Also noted were small amounts of sphalerite and traces of chalcocite, digenite, covellite, and locally abundant goethite.

In thin section the rocks are seen to be fine-grained and highly siliceous; the matrix consists of fine-grained quartz averaging about 20 μm in one specimen, and <50 μm in all. Laths and shreds of fine-grained chlorite are abundant and substantially exceed those of muscovite, thus accounting for the dark megascopic appearance. Anhedral quartz phenocrysts are present in all samples and are generally 0.3-0.6 mm in diameter. These phenocrysts, and rounded to ellipsoidal bodies 1-5 mm across which consist of polycrystalline quartz, make up 50-80% of the sections. A small amount of the mica in one of the specimens has the pleochroic characteristics of phlogopite; electron-microprobe analyses correspond fairly well to this phase and show it to be highly enriched in magnesium (Table A-1). Carbonate (predominantly dolomite) is dispersed throughout two of the thin sections as grains up to 0.25 mm, and makes up an estimated 5-6% of these rocks. Carbonate constitutes only about 2% of the third section, occurring erratically as discontinuous microscopic veinlets and patches, and as scattered minute grains in the matrix.

The chlorite-rich matrix of these rocks contains disseminated angular quartz grains, and the texture resembles that of a tuff. The ovoids and quartz patches give the rock a megascopic resemblance to lapilli tuff. In transmitted light the patches and ovoids are seen to be polycrystalline, and much of the zoning reflects both the crystallographic orientation and the size of quartz grains in specific arrays.

(b) INT 10-49(2)

The bag contained four specimens of about 5 x 6 x 9 cm, plus eight at approximately half this size. The rocks were similar to those in (a) above. Several of the specimens contained fine-grained pyrite and chalcopyrite $\pm$ sphalerite, and the overall sulphide content was probably similar to that of bag (a).

Two polished sections from different hand specimens are unalike. In one, pyrite is more abundant than chalcopyrite, and only traces of sphalerite are present. The pyrite is riddled with poikiloblastic inclusions, and some grains are shattered and healed by chalcopyrite veinlets. In the other section, chalcopyrite is the most abundant sulphide, and it

is accompanied by substantial amounts of pyrite and sphalerite. Total sulphide content is about 4%, which is shared among fine-grained disseminations, hairline veinlets, and relatively coarse pyrite-chalcopyrite patches that exceed 1 mm across. A few of the coarser chalcopyrite grains are slightly altered to goethite(?) and covellite.

Two thin sections of two specimens are similar in having fragmental textures; the fragments are angular but lack sharp edges. Size of the fragments in one section averages about 0.5 cm across, and most are large; in the other section the size is more variable, from millimetres to 0.5 cm. The assemblage consists of equigranular quartz averaging 20 μm across, with abundant chlorite in masses and as a matrix to the fragments (some of which are quartz phenocrysts rather than fragments). Only traces of muscovite occur. Carbonate in one section is in anhedral grains to 0.4 mm across.

CO-DISPOSAL 3

(a) RD BX 48-109

The bag contained 6 pieces averaging about 5 x 9 x 10 cm, plus 6 at 4 x 4 x 5 cm. All except one of the larger pieces were highly siliceous and sulphide-rich (mainly pyrite and sphalerite, with a combined average estimated to be about 5% by volume); the exceptional piece was black, chloritic, pyritiferous, and "non-siliceous" relative to the other specimens.

Four polished sections were prepared from three of the specimens. Sulphide content in the sections is highly variable, ranging from 5% to 40%. Pyrite is predominant, and in the most sulphide-rich specimens about a third of the pyrite consists of disseminated isolated grains, many of them euhedral and riddled with inclusions of gangue, plus a few blebs of chalcopyrite and traces of pyrrhotite. The remaining portion of the sulphides (i.e., two thirds of the total) consists of coarse pyrite grains and aggregates, much containing irregular patches of sphalerite and less abundant galena.

Two of the sections contain 10-15% sulphides, mainly pyrite that ranges from 5 to 200 μm along an edge. Sphalerite, chalcopyrite, and galena occur in lesser amounts at pyrite grain boundaries or as inclusions. All of the sulphides are disseminated or occur in

discontinuous streaks and patches along foliations. In the last of the four polished sections the sulphide content averages about 5%, again mainly as trains of grains along foliation planes. Sphalerite is common, much more so than chalcopyrite and galena, and traces of chalcocite occur as hairline veinlets and rims. The section also contains native silver (Fig. 4).

Although the sample designation is RD BX (rhyodacite breccia), the two thin sections available lack clear-cut indications of brecciation, and appear more akin to tuff fragmentals. The rock is more massive than the preceding co-disposal samples, and is coarser in that the matrix quartz mosaic consists of grains typically 30 to 100 μm across. Muscovite is relatively sparse, which is atypical, and the chief non-sulphide constituents are quartz, chlorite and carbonates. In one of the sections the carbonate mineral content is about 30%; most of the grains are anhedral and 70 to 100 μm across. The other section has less carbonate, and is unusual in that one grain of dolomite-siderite is about 0.8 mm across and is extensively veined by calcite; calcite, however, is extremely sparse in the Selbaie samples, as was indicated by the mainly negative results obtained with the "alizarin red" stain applied to all thin sections. Another unusual feature in co-disposal 3 is the presence of small amounts of disseminated grains of phlogopite (Table A-1); these are similar in size to the associated muscovite and chlorite, among which the phlogopite is disseminated. A few grains of zoned subhedral apatite averaging $\sim 50 \times 90$ μm were observed. Also noted were traces of monazite in grains of a size similar to that of apatite.

(b) RD BX 40-119

The 10 pieces of rock in this bag ranged from about 3 x 7 x 8 cm to 5 x 7 x 12 cm. Pyrite, chalcopyrite, galena and sphalerite were megascopically visible, and all of the rocks were sulphide-rich as in the (a) bag. Quartz "eyes" to 2 cm were locally evident, and the rocks varied from a sulphide-rich "intermediate" phase (as in co-disposal 2) to quartzose "andesite". Some pieces appeared to have a layered structure in which quartz-rich layers about 5 mm thick were separated by chlorite-rich layers about 1 mm thick. The overall

impression was, however, that most of the rock pieces were similar to those of the intermediate phase.

Two polished sections of the specimens were examined. The first is from a specimen that is relatively low in sulphides (~ 10%), but the section itself contains about 70% sulphides, most of which is euhedral to subhedral pyrite up to 400 μm along an edge; galena and sphalerite are common as inclusions and along grain boundaries, but only traces of chalcopyrite are present.

The second section contains about 20% sulphides. These are concentrated mostly along two parallel zones, one 2-3 mm wide and consisting largely of sphalerite, and the other 3-4 mm wide and made up largely of pyrite. Neither of the zones has sharply bounded margins. The sphalerite-rich strip as seen in reflected light has coarse-grained sphalerite with dispersed blebs of chalcopyrite (a relatively coarse-grained "chalcopyrite disease"), pyrite in euhedral grains up to 0.9 mm along an edge, galena as anhedral grains included in sphalerite, and a bleb inclusion of pyrrhotite. The pyrite-rich zone contains minor amounts of sphalerite and lesser galena, mainly as inclusions in pyrite and along its internal grain boundaries.

The sole thin section shows that the bulk of this particular rock contains only 0.2-0.3% sulphides, 99% of which is pyrite, and the remainder is sphalerite. The rock is moderately well foliated and consists largely of ovoid to lensoid bodies that are interpreted to be silicified lapilli. They are typically less than 0.5 cm in long dimension, and consist of fine-grained quartz aggregates; a few of the "ovoids" are quartz phenocrysts rather than lapilli. The matrix of the rock consists of a fine-grained quartz mosaic accompanied by lesser amounts of chlorite and substantially less muscovite. Grain size of the matrix quartz is variable but not significantly different from that of co-disposal 1 or 2. Carbonate minerals are widely disseminated, but the content averages only about 1%.

In summary, the RD BX (rhyodacite breccia) samples are highly variable in sulphide content, are variable in grain size but seemingly not appreciably different from preceding samples, and apparently are locally enriched in carbonates. The specimens could be characterized as lapilli tuff; those examined microscopically are certainly more tuff-like that the rhyodacite breccia illustrated and described by Deptuck et al. (1982).

CO-DISPOSAL 5: PY 0-14 and PY 0-14(2)

Co-disposal 5 consisted of two bags of rocks; one, labelled PY 0-14, contained 14 pieces of rock, the largest of which was 12 x 9 x 7 cm, and the smallest about a quarter that size. Eleven of the 14 pieces were massive sulphides (i.e., >60% sulphides by volume), and the remainder were pyrite-rich (>30% sulphides) and well-layered. The second bag, which was labelled PY 0-14(2), contained 11 pieces of rock in a size range and of a composition similar to those of the rocks in the first bag.

The sample was examined in 9 polished sections and 1 thin section. Individual polished sections have sulphide contents ranging from 40% to 90%. In general, nearly all of the sulphide is pyrite, and the accompanying ore minerals may be characterized as "low-grade", consisting mainly of interstitial sphalerite and traces of chalcopyrite. Much of the pyrite retains vestiges of colloform and radial textures. In the least sulphide-rich sections much of the pyrite is fine-grained and shows circular, atoll, and spherical textures indicative of framboidal pyrite.

The rock examined in thin section contains about 30% pyrite in what megascopically appears to be a quartz-rich, well-bedded tuff. In transmitted light the microscopic textures are characteristic of colloform and framboidal pyrite. The matrix consists of quartz and chlorite (no muscovite), with only traces of carbonate.

Table A-1. Electron-microprobe analyses of Selbaie phlogopite

		"Large" grain	Av. of 3 small		Formula ratios			
		A	B		A		B	
wt%	K_2O	9.9	9.6	K	0.88		0.88	
	MgO	23.9	23.9	Mg	2.48		2.53	
	FeO	5.7	5.5	Fe	0.33	2.84	0.33	2.89
	TiO_2	0.7	0.5	Ti	0.03		0.03	
	Al_2O_3	12.5	12.3	Al	1.00		1.00	
	SiO_2	43.1	41.7	Al	0.03	3.00	0.03	3.00
	sum	94.8	93.5	Si	2.97		2.97	

Table A-2. Electron-microprobe analysis of Fe-rich chlorite

wt%	SiO_2	26.25	Fe^{2+}	6.703	8.000
	Al_2O_3	20.59	Mg	1.297	
	MgO	3.81			
	FeO*	30.39	Fe^{3+}	1.284	
	Fe_2O_3	6.46	Al	5.538	12.000
	sum	87.50	Si	5.178	
			O		20.589
			OH		16.000

*Fe partitioned into FeO and Fe_2O_3 according to formula requirements.